Journal of Organometallic Chemistry, 441 (1992) 309–322
Elsevier Sequoia S.A., Lausanne
JOM 22981

Mixed-valence state of 1′,1‴-dialkylbiruthenocenium(II,IV) salts

Masanobu Watanabe, Toschitake Iwamoto

Department of Chemistry, College of Arts and Sciences, The University of Tokyo, Komaba, Meguro, Tokyo 153 (Japan)

Hirotoshi Sano, Atsushi Kubo

Department of Chemistry, Faculty of Sciences, Tokyo Metropolitan University, Minami-ohsawa, Hachioji, Tokyo 192-03 (Japan)

and Izumi Motoyama

Department of Chemistry, Faculty of Engineering, Kanagawa University, Rokkakubashi, Yokohama 221 (Japan)

(Received February 21, 1992)

Abstract

1′,1‴-Diethylbiruthenocene and 1′,1‴-dipropylbiruthenocene, prepared by the reduction with $LiAlH_4$–$AlCl_3$ of 1′,1‴-diacetylbiruthenocene and 1′,1‴-dipropionylbiruthenocene respectively, are oxidized to give mixed valence halo-1′,1‴-dialkylbiruthenocenium(II,IV) salts formulated as $[Ru^{IV}Cp'(C_5H_4)(C_5H_4)Cp'Ru^{II}X]^+ Y^-$ (X = Cl, Br, I; Y = PF_6, I_3). The temperature dependence of the ^1H NMR spectroscopy of the salts in acetone-d_6 suggests the rate of electron transfer between the Ru^{II} and Ru^{IV} atoms accompanied with exchange of the halogen atom is less than in halobiruthenocenium (II,IV) salts, owing to steric hindrance by the dialkyl groups.

Introduction

In the last two decades, mixed-valence binuclear ferrocene derivatives have been proved a good model for investigation of intramolecular electron transfer. Especially, ^{57}Fe-Mössbauer spectroscopic studies on the mixed-valence 1′,1‴-dialkylbiferrocenium(II,III) salts (ethyl, propyl, and butyl) have revealed a temperature dependence of these spectra, while biferrocenium salts gave merely the trapped-valence spectra in the range 4.2–300 K [1–4]. Dialkyl substitution evidently increases the rate of electron exchange between the Fe^{II} and Fe^{III} atoms in mixed valence 1′,1‴-dialkylbiferrocenium systems.

Correspondence to: Dr. M. Watanabe.

No study on the chemistry of mixed-valence 1,1″-biruthenocene, RcRc, has so far been reported because it has been obtained only in poor yield [5]. Recently, we reported a novel and high-yielding synthesis of RcRc via ruthenocene, RcH, and of its mixed-valence oxidation products such as iodobiruthenocenium(II,IV) triiodide, $[RcRcI]^+I_3^-$ (**1**) and halobiruthenocenium(II,IV) hexafluorophosphate, $[RcRcX]^+PF_6^-$ for X = Br (**2**), Cl, (**3**) salts [6–8]. Although the salts hold trapped valence states at low temperatures, the remarkable temperature dependences of their ^{1}H- and ^{13}C-NMR spectra in acetone-d_6 support the averaging of valence states between the formal Ru^{II} and Ru^{IV} at higher temperatures. Here we describe syntheses of 1′,1‴-diethylbiruthenocene, $RcRcEt_2$, and 1′,1‴-dipropylbiruthenocene, $RcRcPr_2$, and the effect of dialkyl substitution on electron transfer between the Ru^{II} and Ru^{IV} in halo-1′,1‴-dialkylbiruthenocenium(II,IV) salts, investigated by means of ^{1}H NMR spectroscopy in acetone-d_6 (99.5%).

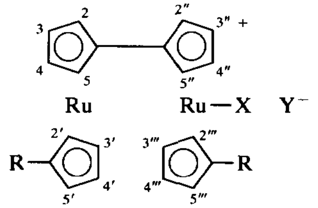

	R	X	Y
1	H	I	I_3
2	H	Br	PF_6
3	H	Cl	PF_6
4	C_2H_5	I	I_3
5	C_2H_5	Br	PF_6
6	C_2H_5	Cl	PF_6
7	C_3H_7	I	$I_3 \cdot 0.5I_2$
8	C_3H_7	Br	PF_6
9	C_3H_7	Cl	PF_6

Experimental

$RcRcEt_2$ was obtained by the reduction of 1′,1‴-diacetylbiruthenocene, $RcRcAc_2$, with $LiAlH_4$–$AlCl_3$, and $RcRcPr_2$ was prepared by a similar method (Scheme 1).

Preparation of 1′,1‴-diacetylbiruthenocene

1′,1‴-Diacetylbiruthenocene was prepared by two methods, firstly, normal acetylation of RcRc with acetyl chloride and boron-trifluoride etherate and secondly, radical coupling of acetylruthenocene, RcAc, in sulphuric acid as applied for RcRc via RcH [7].

(a) 1,1″-Biruthenocene (2.0 g, 4.34 mmol) dissolved in methylene chloride (200 cm^3) was placed in a 3-necked flask. To this solution acetyl chloride (0.7 cm^3) and boron-trifluoride etherate (5.0 cm^3) dissolved in methylene chloride (100 cm^3) were added dropwise at 0°C over a period of 1 h. The reaction mixture was refluxed for 10 h under nitrogen, and poured into an aqueous solution of sodium carbonate. After the reaction mixture was extracted with benzene, the organic phase was washed with dilute hydrochloric acid then with water, dried and

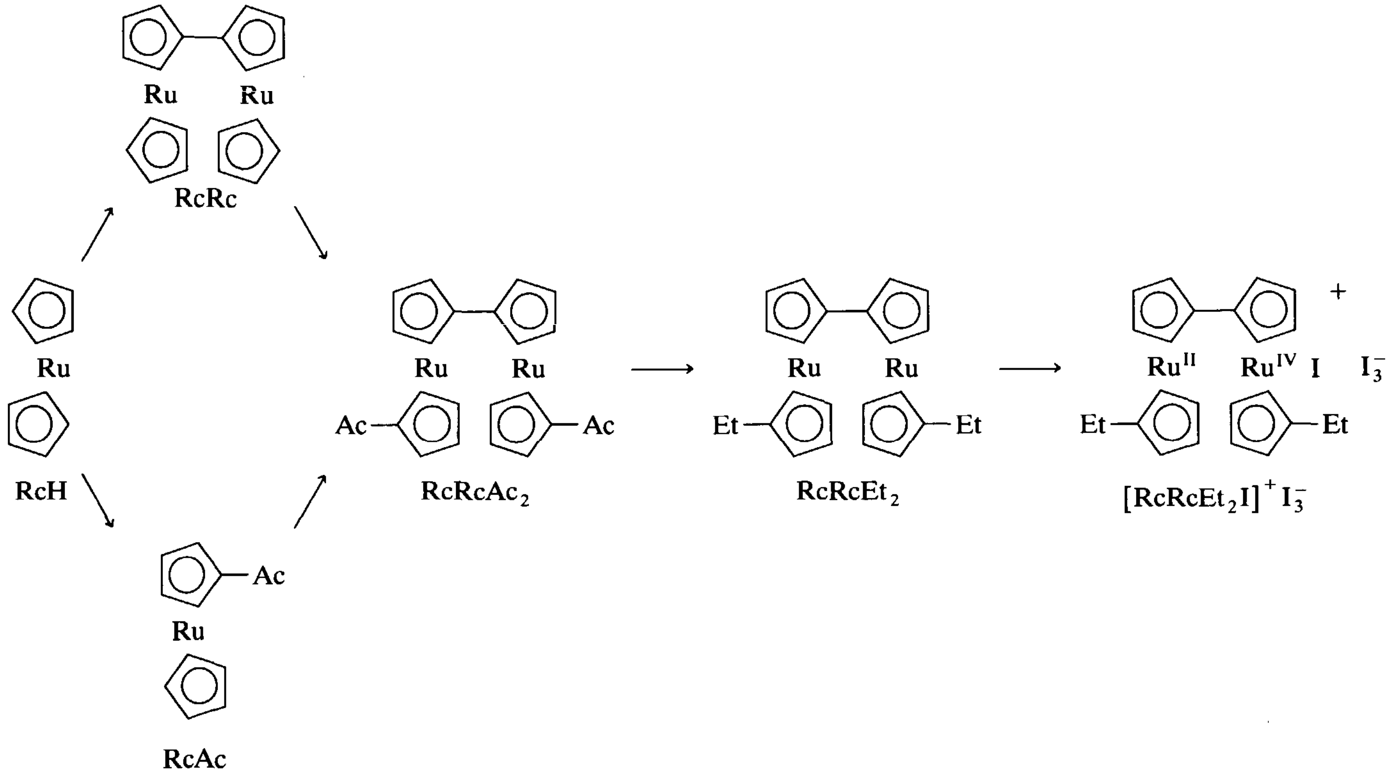
Ru
Ru
RcRc
Ru
RcH
Ac
Ru
RcAc
Ru
Ru
Ac
Ac
RcRcAc$_2$
Ru
Ru
Et
Et
RcRcEt$_2$
+
Ru^{II}
Ru^{IV} I
I_3^-
Et
Et
$[RcRcEt_2I]^+I_3^-$

Scheme 1.

evaporated. Products were purified by column chromatography on alumina (300 mesh). The first fraction eluted with benzene (a pale yellow band) contained RcRc. Monoacetylbiruthenocene, RcRcAc, was then obtained by using a benzene–diethyl ether (2 : 1) mixture. The crude product was recrystallized from a benzene–hexane (2 : 1) mixture to give yellow crystals (1.2 g, 2.39 mmol; yield 55%). Anal. Found: C, 52.38; H, 4.16. $C_{22}H_{20}ORu_2$ calcd.: C, 52.58; H, 4.01%. ^{1}H NMR ($CDCl_3$): δ 5.01 (2H, t, J = 1.8 Hz), 4.73 (2H, t, J = 1.8), 4.70 (2H, t, J = 1.8), 4.68 (2H, t, J = 1.8), 4.50 (4H, t, J = 1.8), 4.47 (5H, s), 2.08 (3H, s) ppm. ^{13}C NMR ($CDCl_3$): δ 201.49 (1C), 91.66 (1C), 87.17 (2C), 87.37 (1C), 76.24 (2C), 73.84 (2C), 73.64 (2C), 73.32 (2C), 73.12 (2C), 72.02 (2C), 71.88 (5C), 28.83 (1C) ppm. The third fraction with a benzene–diethyl ether–methanol (5 : 5 : 1) mixture gave $RcRcAc_2$, which was recrystallized from a benzene–hexane (1 : 1) mixture to give yellow crystals (0.35 g, 0.65 mmol; yield 15%). Anal. Found: C, 53.09; H, 4.02. $C_{24}H_{22}O_2Ru_2$ calcd.: C, 52.93; H, 4.07%. ^{1}H NMR ($CDCl_3$): δ 5.01 (4H, t, J = 1.7 Hz), 4.72 (4H, t, J = 1.7), 4.69 (4H, t, J = 1.7), 4.55 (4H, t, J = 1.7), 2.03 (6H, s) ppm. ^{13}C NMR ($CDCl_3$): δ 201.24 (2C), 89.32 (2C), 87.17 (2C), 76.32 (4C), 73.98 (4C), 73.65 (4C), 72.74 (4C), 28.92 (2C) ppm.

(b) RcAc (1.0 g, 3.7 mmol) was dissolved in sulphuric acid (50 cm^3) at room temperature. After standing for 15 min at 60°C, the solution was poured into ice–water containing $TiCl_3$ (1.0 g). The organic phase was extracted with benzene, washed with water and dried. The crude compounds were purified by alumina-column chromatography. RcAc was first eluted by a mixture of ether–benzene (1 : 1) (0.3 g, 1.1 mmol; 30% recovery). $RcRcAc_2$ was obtained as the second fraction by using a benzene–diethyl ether–methanol (5 : 5 : 1) mixture, and was recrystallized from a benzene–hexane (1 : 1) mixture to give yellow crystals (0.5 g, 0.92 mmol; yield 25%). The purity of the compound was confirmed by elemental analysis, infrared, ^{1}H NMR, and ^{13}C NMR spectroscopies and the results were identical with those prepared as above from acetylation of RcRc.

Preparation of 1′,1‴-diethylbiruthenocene

1′,1‴-Diacetylbiruthenocene (2.0 g, 3.67 mmol) was added to a dry ethereal solution (100 cm^3) containing anhydrous aluminium chloride (5.0 g) and lithium aluminium hydride (2.0 g); the yellow solution immediately lost its colour. After water was added, the reaction mixture was extracted with benzene, and the extract washed with water, dried, and evaporated. $RcRcEt_2$ was separated by alumina-column chromatography using a benzene–hexane (1 : 1) mixture, and was recrystallized from a benzene–hexane mixture to give pale yellow crystals (1.5 g, 2.90 mmol; yield 79%). Anal. Found: C, 55.87; H, 5.09%. $C_{24}H_{26}Ru_2$ calcd.: C, 55.80; H, 5.07%. ^{1}H NMR ($CDCl_3$): δ 4.64 (4H, t, J = 1.6 Hz), 4.45 (4H, t, J = 1.6), 4.41 (4H, t, J = 1.5), 4.36 (4H, t, J = 1.5), 2.07 (4H, q, J = 7.5), 1.00 (6H, t, J = 7.5) ppm. ^{13}C NMR ($CDCl_3$): δ 97.13 (2C), 88.94 (2C), 73.16 (4C), 72.08 (4C), 72.03 (4C), 71.68 (4C), 23.49 (2C), 17.12 (2C).

Preparation of 1′,1‴-dipropionylbiruthenocene and 1′,1‴-dipropylbiruthenocene

1′,1‴-Dipropionylbiruthenocene was prepared in a poor yield (trace) by the radical coupling of propionylruthenocene in sulphuric acid, which proceeded by the reaction of RcRc with propionyl chloride and boron trifluoride etherate in the same conditions as those used for $RcRcAc_2$. 1′1‴-Dipropionylbiruthenocene was recrystallized from a benzene–hexane (1 : 1) mixture to give yellow crystals. Anal. Found: C, 53.59; H, 4.40. $C_{26}H_{26}O_2Ru_2$ calcd.: C, 54.15; H, 4.54%. ^{1}H NMR ($CDCl_3$): 5.01 (4H, t, J = 1.7 Hz), 4.68 (4H, t, J = 1.7), 4.67 (4H, t, J = 1.7), 4.53 (4H, t, J = 1.7), 2.37 (4H, q, J = 7.3), 1.01 (6H, t, J = 7.3). ^{13}C NMR ($CDCl_3$): δ 204.04 (2C), 89.44 (2C), 86.91 (2C), 75.98 (4C), 73.64 (4C), 72.86 (4C), 71.95 (4C), 34.17 (2C), 10.50 (2C) ppm.

The compound $RcRcPr_2$ was prepared by the method used for $RcRcEt_2$. Anal. Found: C, 56.99; H, 5.34. $C_{26}H_{30}Ru_2$ calcd.: C, 57.33; H, 5.55%. ^{1}H NMR ($CDCl_3$): δ 4.62 (4H, t, J = 1.6 Hz), 4.44 (4H, t, J = 1.6), 4.40 (4H, t, J = 1.5), 4.35 (4H, t, J = 1.5), 1.98 (4H, t, J = 7.8), 1.39 (4H, m), 0.87 (6H, t, J = 7.3). ^{13}C NMR ($CDCl_3$): δ 95.25 (2C), 88.94 (2C), 73.16 (4C), 72.07 (4C), 72.03 (4C), 71.68 (4C), 33.00 (2C), 26.60 (2C), 15.25 (2C).

Preparation of iodo-1′,1‴-diethylbiruthenocenium(II,IV)$^+I_3^-$ and other salts

Iodo-1′,1‴-diethylbiruthenocenium(II,IV)$^+I_3^-$, $[RcRcEt_2I]^+I_3^-$ (**4**) and iodo-1′,1‴-dipropylbiruthenocenium(II,IV)$^+I_3^-0.5I_2$, $[RcRcPr_2I]^+I_3^-0.5I_2$ (**7**) salts were prepared by the method applied for **1** [6–8]. Anal. Found: C, 27.95; H, 2.60. $C_{24}H_{26}Ru_2I_4$ calcd.: C, 28.14; H, 2.56%. Anal. Found: C, 26.43; H, 2.28. $C_{26}H_{30}Ru_2I_5$ calcd.: C, 26.48; H, 2.56%. Bromo-1′,1‴-diethylbiruthenocenium(II,IV) hexafluorophosphate, $[RcRcEt_2Br]^+PF_6^-$ (**5**) and chloro-1′,1‴-diethylbiruthenocenium(II,IV) hexafluorophosphate, $[RcRcEt_2Cl]^+PF_6^-$ (**6**) were prepared by a similar method [9]. $RcRcEt_2$ (100 mg; 0.193 mmol) dissolved in 30 ml of CH_2Cl_2 was added to a stoichiometric amount of $RuCp_2XPF_6$ (X = Cl, Br) dissolved in 100 ml of CH_2Cl_2. The reaction mixture was stirred for 30 min and evaporated. $RuCp_2$ was extracted with benzene and the salt (**5**, **6**) was recrystallized from a CH_2Cl_2–C_6H_{14} mixture to give red purple crystals. Anal. Found: C, 38.90; H, 3.43. $C_{24}H_{26}Ru_2BrPF_6$ calcd.: C, 38.87; H, 3.53%. Anal. Found: C, 40.71; H, 3.56. $C_{24}H_{26}Ru_2ClPF_6$ calcd.: C, 41.35; H, 3.76%.

Bromo-1′,1‴-dipropylbiruthenocenium(II,IV)$^+$ hexafluorophosphate, $[RcRcPr_2Br]^+PF_6^-$ (**8**) and chloro-1′,1‴-dipropylbiruthenocenium(II,IV)$^+$ hexafluorophosphate, $[RcRcPr_2Cl]^+PF_6^-$ (**9**) were prepared by the methods used for **5** and **6**, respectively. Anal. Found: C, 42.23; H, 3.99. $C_{26}H_{30}Ru_2ClPF_6$ calcd.: C, 43.07; H, 4.17%. Anal. Found: C, 39.62; H, 4.16. $C_{26}H_{30}Ru_2BrPF_6$ calcd.: C, 40.58; H, 3.93%.

NMR, electronic spectroscopy and cyclic voltammogram

^{1}H NMR spectra of **1** and related compounds in acetone-d_6 were recorded on a JEOL FX-90Q spectrometer at 89.59 MHz using TMS as a standard. An NM–VTS unit was used to control the probe temperatures within ±1°C. The assignment of the signals of the $RcRcEt_2$ and related compounds were by selective proton-decoupling experiments. The simulated spectra were calculated using the model of chemical exchange between two equivalent sites proposed by Abragam [10]. Electronic spectra were measured in acetonitrile with a Hitachi spectrophotometer Model 220 at room temperature. Cyclic voltammograms were obtained with an HB-104 function generator and HA-301 potentiostat (Hokuto Denko) with standard three-electrode configuration. A working electrode (platinum button) and an Ag/AgCl reference electrode were connected via a salt bridge of CH_3CN containing $[(C_4H_9)_4N]ClO_4$ (0.1 mol dm^{-3}). The scan rate was 100 mV s^{-1}.

Results and discussion

Preparation of 1′,1‴-diacetylbiruthenocene

As mentioned in the Experimental section, $RcRcAc_2$ was prepared by two methods, the acetylation of RcRc with CH_3COCl and BF_3–Et_2O, and the radical coupling of RcAc in sulphuric acid (Scheme 1). In the former method the yield of $RcRcAc_2$ was poor (15%) and RcRcAc was a main product. $RcRcAc_2$ was also prepared by using $AlCl_3$ as a Lewis acid instead of BF_3–Et_2O together with RcRcAc and polyacetylbiruthenocenes (di-, tri-, tetra- and so on), but only a small amount of $RcRcAc_2$ (3–5%) was separated on alumina-column chromatography. On the other hand, $RcRcAc_2$ was given exclusively by the latter reaction because it could be separated easily from the starting material.

By analogy with the preparation of RcRc from RcH via radical coupling, the latter reaction is assumed to proceed as follows [7]; RcAc gives radical cations, $[(C_5H_4COCH_3)(C_5H_4^{\cdot})Ru^{II}]^+$, in sulphuric acid at 60°C, and coupling of the radical gives dications, $[Ru^{II}(C_5H_4COCH_3)(C_5H_4^{\cdot})(C_5H_4^{\cdot})(C_5H_4COCH_3)Ru^{II}]^{2+}$. The dication gives $RcRcAc_2$ by reduction with $TiCl_3$. In the case of $RcRcEt_2$, the radical reaction of ethylruthenocene under the same conditions was unsuccessful and the starting material was recovered. Evidently ethylruthenocene may be oxidized in sulphuric acid to give a ruthenocenium cation only. Cyclic voltammography of acetylruthenocene in acetonitrile shows one irreversible two-electron oxidation peak and $E_{1/2}$ in acetonitrile is found to be 0.82 V, much higher than that for ruthenocene (0.67 V) and for ethylruthenocene (0.64 V) (present study). The reason why RcAc gives the radical cation and ethylruthenocene gives the ethylruthenocenium cation is considered to be the much higher oxidation potential of the Ru atoms in the former caused by the acetyl group on the terminal Cp ring.

Compounds 4 and 7

The effect of the alkyl groups on electron transfer between the Ru^{II} and Ru^{IV} in halo-1′,1‴-dialkylbiruthenocenium salts is indicated by the temperature dependent 90 MHz ^1H NMR spectra of **1**, **4** and **7** in CD_3COCD_3, shown with their computer simulation in Figs. 1 and 2. The ^1H chemical shifts (δ) are listed in Table 1. Although those of **4** and **7** are more complicated than those of **1** due to the ethyl and propyl groups, these spectra exhibit remarakble temperature dependences supporting the hypothesis that there is electron transfer between the Ru^{II} and Ru^{IV} atoms in **1**; *i.e.*, the Ru^{II}–Ru^{IV} trapped valence state at 183 K turns to the averaged valence state as temperature increases.

The unbalanced trapped valence state of **4** is reflected by the spectrum observed at 183 K. By analogy with the spectrum of **1**, the eight sharp bands in the 4–7 ppm region are assigned as follows: 6.41 (2H), 5.90 (2H) ppm to the Cp ring protons of $H_{2'',5''}$ and $H_{3'',4''}$; 6.11 (2H) and 5.95 (2H) ppm to those of $H_{2''',5'''}$ and $H_{3''',4'''}$; 5.39 (2H) and 5.21 (2H) ppm to those of $H_{2,5}$ and $H_{3,4}$; 4.65 (2H) and 4.53 (2H) ppm to those of $H_{2',5'}$ and $H_{3',4'}$. The methyl (δ 1.00) and methylene signals of the ethyl groups also suffer the effect of the unbalanced valence states of the Ru atoms. The signal centred at 2.56 ppm is assigned to the methylene protons at the Ru^{IV} side, while the signal of those at the Ru^{II} side overlaps with the strong signals of acetone in acetone-d_6 (99.5%). The salt is concluded to take the trapped-valence state $[Ru^{II}(C_5H_4C_2H_5)(C_5H_4)(C_5H_4)(C_5H_4C_2H_5)Ru^{IV}]^+I_3^-$. The lower chemi-

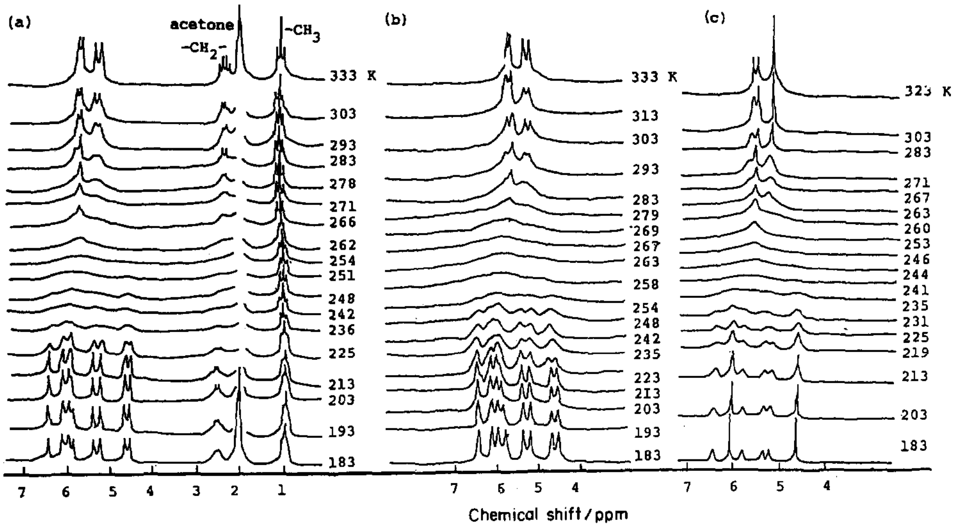

Fig. 1. Temperature-dependent 90 MHz ^1H NMR spectra of **4** (a), **7** (b) and **1** (c) at indicated temperature.

cal shifts of the Ru^{IV} side compared with those of the Ru^{II} side are due to formation of the Ru^{IV}–I bond [11].

Upon heating, the Cp bands broaden, and the coalescence temperature, T_c, for the $H_{2',5'}$, $H_{3',4'}$ and $H_{2''',5'''}$, $H_{3''',4'''}$ is given as about 256 ± 1 K. Above T_c, the bands due to the Cp, methylene, and methyl protons get sharper with no difference in chemical shift between the Ru^{II} and Ru^{IV} sides; the bands at 5.71 and 5.67 ppm are assigned to the Cp ring protons of $-(C_5H_4)-$, 5.34 and 5.21 ppm to those of $-(C_5H_4C_2H_5)$, 2.33 ppm to $-CH_2-$ and of 1.08 ppm to $-CH_3$ of the ethyl groups at 333 K.

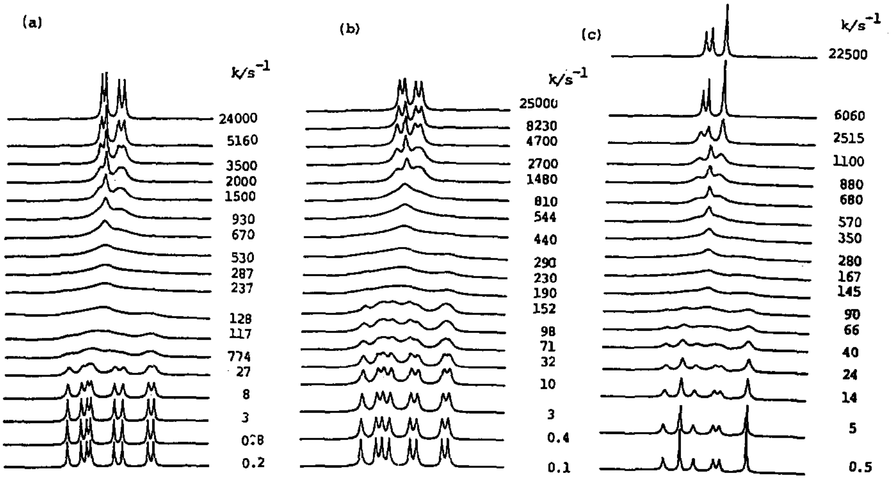

Fig. 2. Calculated ^1H NMR spectra of **4** (a), **7** (b) and **1** (c).

Table 1

^1H chemical shifts of RcRc and related compounds at indicated temperatures

Compound	Temp. (K)	Chemical shifts (ppm)	
RcRc [a]	298	4.68, 4.44, 4.48	
1	183	6.41, 5.76, 6.05	$[(C_5H_4)(C_5H_5)Ru^{IV}I]^+$
		5.33, 5.19, 4.61	$(C_5H_4)(C_5H_5)Ru^{II}$
	323	5.72, 5.62, 5.30	
4	183	6.41, 6.11, 5.95, 5.90	$[(C_5H_4)(C_5H_4C_2H_5)Ru^{IV}I]^+$
		5.39, 5.21, 4.65, 4.53	$(C_5H_4)(C_5H_4C_2H_5)Ru^{II}$
		2.56 ($-CH_2-$), 1.00 ($-CH_3$)	
	333	5.71, 5.67, 5.34, 5.21	
		2.30 ($-CH_2-$), 1.08 ($-CH_3$)	
5	183	6.34, 5.88, 5.71	$[(C_5H_4)(C_5H_4C_2H_5)Ru^{IV}Br]^+$
		5.29, 4.72, 4.61	$(C_5H_4)(C_5H_4C_2H_5)Ru^{II}$
		2.53 ($-CH_2-$), 0.98 ($-CH_3$)	
	303	5.75, 5.44, 5.23	
		2.30 ($-CH_2-$), 1.07 ($-CH_3$)	
6	178	6.32, 5.88, 5.76	$[(C_5H_4)(C_5H_4C_2H_5)Ru^{IV}Cl]^+$
		5.29, 4.74, 4.63	$(C_5H_4)(C_5H_4C_2H_5)Ru^{II}$
		2.53 ($-CH_2-$), 0.98 ($-CH_3$)	
	271	5.77, 5.41, 5.21	
		2.31 ($-CH_2-$), 1.08 ($-CH_3$)	
7	183	6.44, 6.11, 5.98, 5.82	$[(C_5H_4)(C_5H_4C_3H_7)Ru^{IV}I]^+$
		5.37, 5.23, 4.67, 4.54	$(C_5H_4)(C_5H_4C_3H_7)Ru^{II}$
		2.50–2.31 ($-CH_2-$), 1.44–1.30 ($-CH_2-$), 0.88 ($-CH_3$)	
	333	5.74, 5.66, 5.36, 5.23	
		2.30 ($-CH_2-$), 1.51 ($-CH_2-$), 0.91 ($-CH_3$)	
8	183	6.36, 5.89, 5.66	$[(C_5H_4)(C_5H_4C_3H_7)Ru^{IV}Br]^+$
		5.28, 4.72, 4.60	$(C_5H_4)(C_5H_4C_3H_7)Ru^{II}$
		2.52–2.34 ($-CH_2-$), 1.54–1.37 ($-CH_2-$), 0.82 ($-CH_3$)	
	293	5.75, 5.41, 5.23	
		2.21 ($-CH_2-$), 1.51 ($-CH_2-$), 0.92 ($-CH_3$)	
9	183	6.32, 5.88, 5.76, 5.69	$[(C_5H_4)(C_5H_4C_3H_7)Ru^{IV}Cl]^+$
		5.27, 4.75, 4.62	$(C_5H_4)(C_5H_4C_3H_7)Ru^{II}$
		2.60–2.30 ($-CH_2-$), 1.51–1.41 ($-CH_2-$), 0.87 ($-CH_3$)	
	293	5.75, 5.38, 5.21	
		2.13 ($-CH_2-$), 1.50 ($-CH_2-$), 0.92 ($-CH_3$)	

[a] RcRc in chloroform solution, the others in acetone

The lifetime τ for the $H_{2'-5'}$, $H_{2'''-5'''}$ signals is estimated to be 3.47 ms at T_c from the equation $\tau = 2^{0.5}/\pi\Delta\delta$, where $\Delta\delta$ (Hz) is the difference in the chemical shifts for signals at 183 K. The Gibbs free energy of activation at T_c, $\Delta G^‡(T_c)$, is calculated as 49.9 ± 0.2 kJ mol^{-1} from the reported calculation [8,12].

As shown in Fig. 1b, similar spectra are observed also for **7**; *i.e.*, the groups of eight and four sharp signals are observed at 183 and 333 K, respectively, in the 4–7 ppm region. Because these peak positions correspond well to those of **4**, the assignment of the peaks for **7** may be identical with those of **4**. Although four kinds

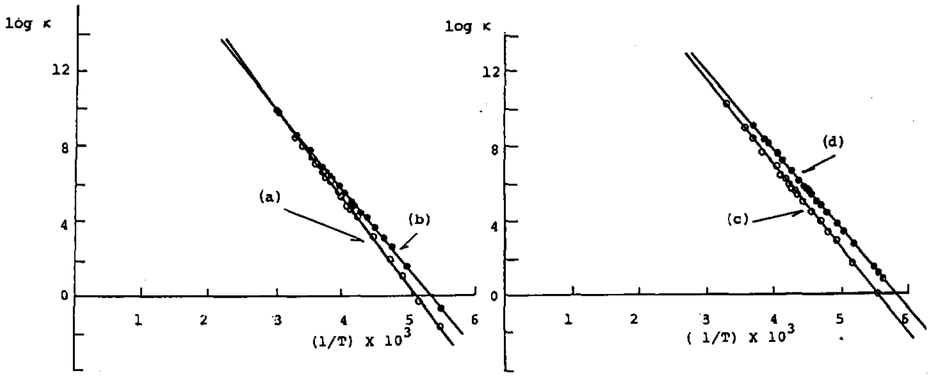

Fig. 3. Arrhenius plot of log κ *versus* $1/T$ of **4** (a), **1** (b), **5** (c) and **6** (d).

of $-CH_2-$ (2 peaks for Ru^{IV} side and 2 peaks for Ru^{II} side) and two kinds of $-CH_3$ signals (one for Ru^{IV} and the other for Ru^{II} side) should be observed in the 2.5–1.3 and 0.8–1.1 ppm regions at 183 K, two kinds of broad $-CH_2-$ and one kind of $-CH_3$ signal (2.50–2.31, 1.44–1.30 and 0.88 ppm) are observed because of the small chemical shift difference between $-CH_2-$ and $-CH_3$ groups of the unbalanced Ru^{II} and Ru^{IV} sides and spin–spin interaction of $-CH_2-$ and $-CH_3$. As in the case of **4**, these signals sharpen at higher temperatures. Slightly longer τ (3.47 ms), higher T_c (263 K) and larger $\Delta G^{\ddagger}(T_c)$ (51.8 ± 0.2 kJ mol^{-1}) are also found for **7** compared to **4**, which suggests the rate of the electron transfer of **7** decreases compared with that of **4**.

In order to estimate the values of T_c, τ and $\Delta G^{\ddagger}(T_c)$ for **1**, temperature dependent 90 MHz ^1H NMR spectroscopy was carried out, as shown in Fig. 1c. As shown in our previous reports on ^1H NMR spectra of **1** at 200 MHz, six and three sharp lines are observed at 183 and 323 K, respectively. The T_c of the main signals is given as *ca.* 246 K for 90 MHz (T_c: 253 K at 200 MHz ^1H NMR) and τ and $\Delta G^{\ddagger}(T_c)$ are estimated to be 3.47 ms and 48.3 ± 0.2 kJ mol^{-1} (1.56 ms and 48.0 ± 0.2 kJ mol^{-1} at 200 MHz ^1H NMR, respectively) [8]. The larger $\Delta G^{\ddagger}(T_c)$ and T_c for **4** and **7** compared with those of **1** suggest the electron transfer between the Ru^{II} and Ru^{IV} for **4** and **7** is retarded.

The computer simulation of the temperature-dependent spectra of the salts (**1**, **4**, **7**) is shown in Fig. 2, in the 4–7 ppm regions, using the modified Bloch equation to obtain the activation parameter. The activation energy, E_a, for **4** was obtained in the usual way from plots of log κ *vs.* T^{-1} (see Fig. 3a). Good linear plots were obtained and the error based on least-squares fitting of the data. The activation energy, E_a, Gibbs free energy of activation $\Delta G^{\ddagger}$, and enthalpy of activation $\Delta H^{\ddagger}$, for **4** are found to be 39.2 ± 0.6, 52.2 ± 0.2 and 36.7 ± 0.6 kJ mol^{-1} (Table 2). Good linear plots were also obtained for **1** in Fig. 3b, the slope of the line is smaller than that for **4**, suggesting E_a, $\Delta G^{\ddagger}$ and $\Delta H^{\ddagger}$ are smaller for **1**. The plots for **7** give the largest E_a, $\Delta G^{\ddagger}$ and $\Delta H^{\ddagger}$. Therefore, the rate of electron exchange between the two Ru atoms in these salts increases in the order **7** < **4** < **1**.

As mentioned in our previous report, the most interesting phenomenon of the mixed-valence halobiruthenocenium(II,IV) salts is observed in their electronic spectra; *i.e.*, a new and strong absorption band appears at *ca.* 480 nm for the

Table 2

Activation parameters for **1** and related compounds from 90 MHz ^1H NMR spectroscopy at 298 K

Compound	T_c (K)	E_a (kJ mol^{-1})	$\Delta G^\ddagger$ (kJ mol^{-1})	$\Delta H^\ddagger$ (kJ mol^{-1})	$\Delta S^\ddagger$ (e.u.)
1	246 ± 1	36.5 ± 0.6	49.1 ± 0.2	34.0 ± 0.6	− 12.1 ± 0.7
2	215 ± 1	34.0 ± 0.5	46.8 ± 0.3	31.5 ± 0.5	− 12.2 ± 0.6
3	207 ± 1	32.8 ± 0.5	45.5 ± 0.2	30.3 ± 0.5	− 12.1 ± 0.5
4	256 ± 1	39.2 ± 0.6	52.2 ± 0.2	36.7 ± 0.6	− 12.4 ± 0.6
5	230 ± 1	37.4 ± 0.5	48.6 ± 0.2	34.9 ± 0.5	− 10.3 ± 0.6
6	215 ± 1	35.2 ± 0.4	47.3 ± 0.2	32.7 ± 0.4	− 11.7 ± 0.5
7	263 ± 1	42.0 ± 0.6	52.7 ± 0.2	39.5 ± 0.6	− 10.6 ± 0.7
8	234 ± 1	39.2 ± 0.5	48.0 ± 0.2	36.7 ± 0.5	− 9.0 ± 0.6
9	230 ± 1	38.0 ± 0.5	45.6 ± 0.2	35.5 ± 0.5	− 8.1 ± 0.6

mixed-valence binuclear system **1** in acetonitrile [8]. The two strong bands assigned as I_3^- are observed at 291 and 362 nm, and the new band is also observed at 490sh nm for **4**. Similarly, three bands (292, 363, and 490sh nm) are also observed for **7**. Probably because of the electron donating effect of the alkyl group (ethyl, propyl), a red shift (10 nm) of the new band is observed for the two salts.

All the results obtained in the present studies suggest the presence of an electron exchange reaction between the two Ru atoms in $[RcRcR_2I]^+I_3^-$ salts ($R = H$, C_2H_5, C_3H_7), with the rate increasing in the order **7** < **4** < **1**.

Compounds 5, 6, 8 and 9

In order to compare the activation parameters for **5**, **6**, **8** and **9** with those of **4** and **7**, the same spectral studies were carried out, and Fig. 4 shows the temperature dependent ^1H NMR spectra of salts **5** and **6**, and Fig. 5 their computer simulation. In the spectrum of **5**, six sharpened bands are observed at 183 K in the 4–7 ppm region. Based on the spectral simulation for **5** and the assignment of the spectra for **2**, the lines are assigned as follows: 6.34 and 5.71 ppm to the protons of $H_{2'',5''}$, $H_{3'',4''}$, 5.88 ppm to $H_{2''',5'''}$, $H_{3''',4'''}$, 5.29 ppm to $H_{2,5}$, $H_{3,4}$ and 4.72 and 4.61 ppm to $H_{2',5'}$, $H_{3',4'}$. As in the case of **4**, the methyl and methylene peaks are observed at 2.53 and 0.98 ppm.

Upon heating of the sample, these lines broaden. T_c for the $H_{2'-5'}$, $H_{2'''-5'''}$ protons is *ca.* 230 K, lower than that for **4** (256 K), and higher than that for **2** (215

Table 3

Electronic spectral data for **1** and related compounds in CH_3CN (250–900 nm)

Compound	λ_{max}(nm) (ϵ in parentheses)
1	290(13200), 360 (8520), 480sh (1590)
2	335(8920), 480 (5600)
3	340(12500), 470 (7080)
4	291(20900), 362 (12900), 490sh (2400)
5	357(9970), 491 (6610)
6	348(12020), 484 (7590)
7	292(19900), 363 (12000), 490sh (2400)
8	363(8120), 492 (5250)
9	348(10470), 483 (6600)

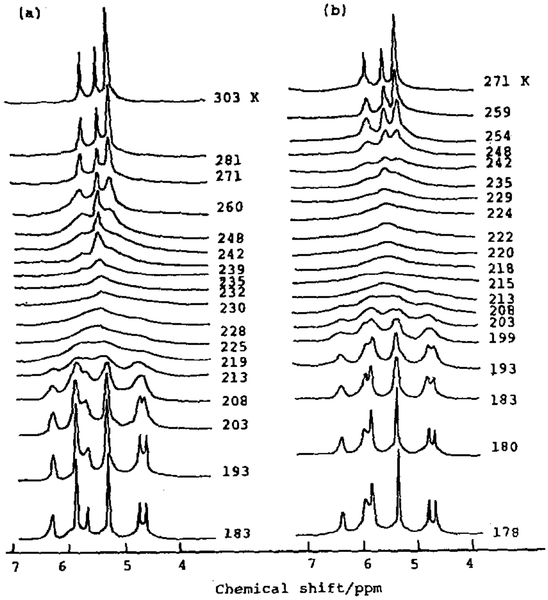

Fig. 4. Temperature-dependent 90 MHz ^{1}H NMR spectra of **5** (a) and **6** (b) at indicated temperatures.

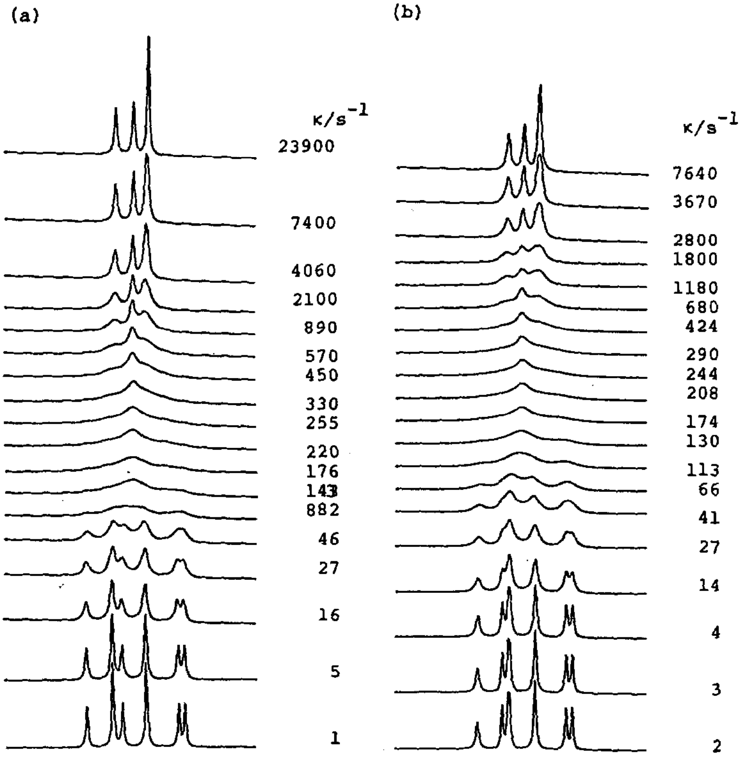

Fig. 5. Calculated ^{1}H NMR spectra of **5** (a) and **6** (b).

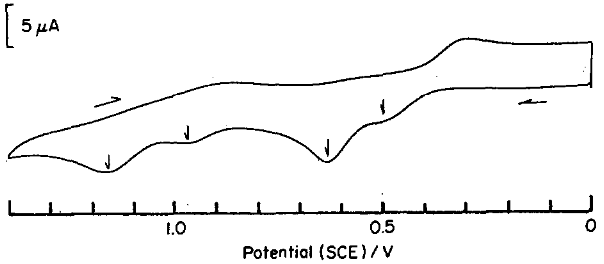

Fig. 6. Cyclic voltammograms of RcRc in acetonitrile. (Sweep rate: 100 mV s^{-1}.)

K). At 303 K, three new sharpened lines are observed. Good linear plots of log κ *vs.* T^{-1} are obtained (Fig. 3c) and E_a, $\Delta G^‡$ and $\Delta H^‡$ are found to be 37.4 ± 0.5, 48.6 ± 0.2 and 34.9 ± 0.5 kJ mol^{-1}, respectively.

Similar spectral features are observed for **6**. Based on the results of spectral simulation for **6**, the lines are assigned as follows: 6.32 and 5.76 ppm to $H_{2'',5''}$, $H_{3'',4''}$, 5.88 and 5.76 ppm to $H_{2''',5'''}$, $H_{3''',4'''}$, 5.29 ppm to $H_{2,5}$, $H_{3,4}$, and 4.74 and 4.63 ppm to $H_{2',5'}$, $H_{3',4'}$. At 271 K, three new sharpened lines are observed. T_c for the $H_{2'-5'}$, $H_{2'''-5'''}$ protons is 215 K, and E_a, $\Delta G^‡$, $\Delta H^‡$ are 35.2 ± 0.4, 47.3 ± 0.2 and 32.7 ± 0.4 kJ mol^{-1}, respectively (Fig. 3d). T_c, E_a, $\Delta G^‡$ and $\Delta H^‡$ for **6** are smaller than for **4** and **5**, suggesting the rate of electron exchange between the Ru^{II} and Ru^{IV} atoms increases in the order **4** < **5** < **6**.

The same was found for **8** and **9**. T_c is 234 and 230 K for **8** and **9** respectively, much lower than that for **7** (263 K) and higher than for **2**, **3**, **5** and **6**. E_a, $\Delta G^‡$ and $\Delta H^‡$ are 39.2 ± 0.5, 48.0 ± 0.2 and 36.7 ± 0.5 kJ mol^{-1} for **8** and 38.0 ± 0.5, 45.6 ± 0.2 and 35.5 ± 0.5 kJ mol^{-1} for **9**, suggesting the rate increases in the order of **7** < **8** < **9**. Moreover, the parameters of the $[RcRcPr_2X]^+PF_6^-$ salts are larger than for corresponding $[RcRcEt_2X]^+PF_6^-$ and $[RcRcX]^+PF_6^-$ salts, suggesting a lower rate of electron exchange between the Ru^{II} and Ru^{IV} in $[RcRcPr_2X]^+PF_6^-$ than in $[RcRcR_2X]^+PF_6^-$ (R: H, C_2H_5), probably because of steric hindrance of the propyl group.

This speculation was confirmed as follows. Cyclic voltammography of RcRc shows four irreversible one-electron oxidation peaks (E_{ox}: 0.48, 0.63, 0.96 and 1.16 V, Fig. 6), whereas RcH in acetonitrile shows one irreversible two-electron oxidation peak. The first oxidation peak on RcRc has therefore been attributed to the oxidation of RcRc to $RcRc^+$ and the second, third and fourth peaks to those of $RcRc^+$ to $RcRc^{2+}$, $RcRc^{2+}$ to $RcRc^{3+}$ and $RcRc^{3+}$ to $RcRc^{4+}$, respectively. Although the same four peaks are found for $RcRcEt_2$, E_{ox} values are slightly smaller (E_{ox}: 0.46, 0.58, 0.91 and 1.11 V) compared to those for RcRc, because of the electron donor effect of the ethyl group. $RcRcPr_2$ gives four E_{ox} peaks (E_{ox}: 0.46, 0.58, 0.93 and 1.12 V) and the values correspond well to those of $RcRcEt_2$; *i.e.*, electron donor effects of ethyl and propyl on the Ru atom are approximately equal. For this reason, E_a values of $RcRcPr_2X^+$ systems are larger than those of $RcRcEt_2X^+$ and $RcRcX^+$ not because of the electronic effect on the Ru atoms, but more probably of the steric hindrance of propyl group of $RcRcPr_2$.

Electron transfer is already associated with exchange of the X atoms between the RcH and $RcHX^+$ species [9,13,14]. The exchange rate is ranked thus:

RcH/RcHI$^+$I$_3^-$> RcH/RcHBr$^+$PF$_6^-$> RcH/RcHCl$^+$PF$_6^-$. The E_a values for the RcH/RcHBr$^+$PF$_6^-$ and RcH/RcHCl$^+$PF$_6^-$ systems (41.7 ± 0.6 and 47.9 ± 0.6 kJ mol^{-1} respectively) are found to be much larger compared with those of binuclear Br and Cl systems [13]. The order is quite different from that for binuclear biruthenocenium systems. Moreover, mononuclear RcHX$^+$PF$_6^-$/RcH systems give green–yellow solutions in acetonitrile, while binuclear RcRcR$_2$X$^+$ (R: H, Et, Pr) systems give deep red–purple solutions; *i.e.*, new absorption bands are found in the range 480–490 nm (**5**: λ_{max} 491 nm; **6**: 484 nm; **8**: 492 nm; **9**: 483 nm). The assignment of the band, however, is at present unknown. It could be deeply concerned with the strong interaction between the Ru^{II} and Ru^{IV} in mixed valence binuclear system. The reason for the difference between mononuclear and binuclear systems may be a difference in the mechanism of intra- or intermolecular electron exchange associated with the halogen atom, between the Ru^{II} and Ru^{IV} atoms. This should result in E_a for the RcRcR$_2$Cl systems (R: H, Et, Pr) being smaller than those of the Br and I systems.

At 183 K for **6** and **9** the chemical shift of H$_{2'-5'}$ (average of 4.74 and 4.63 ppm) differs from that of H$_{2'''-5'''}$ (average of 5.88 and 5.76 ppm) by 1.13 ppm ($\Delta\delta$). For **3** the difference is 1.19 ppm. $\Delta\delta$ is larger for the Br systems (1.25, 1.22 and 1.23 ppm for **2**, **5** and **8**) and the I systems (1.44 ppm for **1**, **4** and **7**) than for the Cl systems. The smaller $\Delta\delta$ of Cl systems indicate smaller chemical shift difference of the Ru^{IV} and Ru^{II} sides compared with those of the Br and I systems. It may be speculated that the smaller ionic radius of Cl$^-$ leads to less distortion of the intermediate cation, [Cp′(C$_5$H$_4$)Ru ⋯ Cl ⋯ Ru(C$_5$H$_4$)Cp′]$^{2+}$, giving smaller E_a and lower T_c values compared with the corresponding Br and I salts.

The results of the present study suggest that there occurs an intramolecular electron exchange reaction between the Ru^{II} and Ru^{IV} atoms in halobiruthenocenium(II,IV) systems. Activation parameters of the reaction are ranked thus, [RcRcPr$_2$X]$^+$Y$^-$> [RcRcEt$_2$X]$^+$Y$^-$> [RcRcX]$^+$Y$^-$ (X = Cl, Br, I; Y = PF$_6$, I$_3$), probably because of steric hindrance of alkyl groups. Compared with the case of the biferrocenium system, where the intramolecular electron transfer between the Fe^{II} and Fe^{III} is accelerated by the effect of ethyl and propyl groups on the Cp ring, the transfer of electrons between Ru^{II} and Ru^{IV} is retarded in the biruthenocenium system. This may be due to the difference in the electron transfer mechanism between the biferrocenium and the biruthenocenium systems. In the former electron transfer takes place through the conjugated –(C$_5$H$_4$)(C$_5$H$_4$)–, while the transfer should be accompanied with a halogen-mediated reaction in the latter; expressed as [XRu^{IV}Cp′(C$_5$H$_4$)(C$_5$H$_4$)Cp′Ru^{II}]$^+$ $\rightleftharpoons$ [Ru^{II}Cp′(C$_5$H$_4$)(C$_5$H$_4$)Cp′Ru^{IV}X]$^+$. The presence of the ethyl and propyl groups on the terminal Cp group may cause steric hindrance for the halogen exchange.

References

1 M.H. Morrison, Jr. and D.N. Hendrickson, Inorg. Chem., 14 (1975) 2331.

2 S. Iijima, R. Saida, I. Motoyama and H. Sano., Bull. Chem. Soc. Jpn., 54 (1981) 1375; S. Nakashima and H. Sano, Bull. Chem. Soc. Jpn., 62 (1989) 3012.

3 S. Nakashima, Y. Masuda, I. Motoyama and H. Sano, Bull. Chem. Soc. Jpn., 60 (1987) 1673. S. Nakashima, M. Katada, I. Motoyama and H. Sano., Bull. Chem. Soc. Jpn., 60 (1987) 2253.

4 S. Nakashima, K. Nishimori, Y. Masuda, H. Sano and M. Sorai, J. Phys. Chem. Solids, 52 (1991) 1169; T.Y. Dong, D.N. Hendrickson, K. Iwai, M.J. Cohn, S.J. Geib, A.L. Rheingold, H. Sano, I. Motoyama and S. Nakashima, J. Am. Chem. Soc., 107 (1985) 7996.

5 E.W. Neuse and M.S. Loonat, Transition Met. Chem., 6 (1981) 260.
6 M. Watanabe, H. Sano and I. Motoyama, Chem. Lett., (1990) 1667.
7 M. Watanabe, S. Kawata, H. Sano, and I. Motoyama, J. Organomet. Chem., 399 (1990) 301.
8 M. Watanabe, T. Iwamoto, S. Kawata, A. Kubo, H. Sano and I. Motoyama, Inorg. Chem., 31 (1992) 177.
9 T.P. Smith, D.J. Iverson, M.W. Droege, K.S. Kwan and H. Taube, Inorg. Chem., 26 (1987) 2882.
10 A. Abragam, The Principles of Nuclear Magnetism, Oxford University Press, London, 1961, Chapter 10, p 447.
11 M. Watanabe and H. Sano, Bull. Chem. Soc. Jpn., 63 (1990) 1455.
12 S. Glastone, K.J. Laidler, H. Eyring, The Theory of Rate Process, McGraw-Hill, London, 1941, Chapter 1.
13 M. Watanabe and H. Sano, Chem. Lett., (1991) 555.
14 K. Kirchner, H.W. Dodgen, S. Wherland and J.P. Hunt, Inorg. Chem., 29 (1990) 2381.